This article has been accepted for publication in IEEE Access. This is the author's version which has not been fully edited and content may change prior to final publication. Citation information: DOI 10.1109/ACCESS.2022.3194887

Date of publication xxxx 00, 0000, date of current version xxxx 00, 0000.

Digital Object Identifier 10.1109/ACCESS.2017.DOI

ASTRE : Prototyping Technique for Modular Soft Robots with Variable Stiffness

JEFFERSON PARDOMUAN[1], NOBUHIRO TAKAHASHI[1], AND HIDEKI KOIKE.[1]
[1]Tokyo Institute of Technology, Tokyo 152-8550, Japan

Corresponding author: Jefferson Pardomuan (e-mail: jefferson.pardomuan@gmail.com).

ABSTRACT Soft robots are advantageous for human interaction because of their adaptability and safe interactivity. However, soft robots research entry is challenging due to the complex fabrication process of elastomeric materials with multiple channels. In this paper, we introduce a prototyping technique for fabrication-friendly soft robots using pneumatic artificial muscle(PAMs) and modular 3D printed reinforcement. We present three primitive deformation structures including bending, twisting, and contracting. Moreover, we propose a novel variable stiffness technique, altering PAMs contraction and radial expansion behavior into locking, malleable, and rotational brake features. We explore both the parallel and series arrangement of the reinforcement module, and we propose new kinds of mixing configurations and scaling techniques. We quantitatively verify the force scaling technique on different types of features. We demonstrate the feasibility of this prototyping technique through six application examples and conclude with a discussion of our research limitations and possible future improvements.

INDEX TERMS Soft robotics, fabrication, shape control, rigidity, modular construction, deployable structures.

I. INTRODUCTION

SOFT robots is advantageous compared with the traditional rigid robot considering human interaction safety and environment adaptability. Soft robot also has other merits such as being lightweight, low energy consumption, and motions that emulate biology. Whitesides et al. describe that in the future soft robots will hold an important role as intermediaries between humans, rigid robots, and computer systems [1]. A variety of potential applications of soft robots are including locomotion, manipulation, and human-machine interaction.

Recently, many solutions for soft robot fabrication have been proposed, however, the majority of soft robots research is built using elastomeric materials such as silicone rubbers [2]. Common techniques include mixing polymer and catalyst, degassing, molding, and adhesion of different layers. This sequence of processes is difficult because experience and know-how are needed to handle issues, such as removing air bubbles and molding small air channels. To cope with this drawback, we proposed a soft robot prototyping technique using pneumatic artificial muscle(PAMs) as a soft actuator, and 3D printed structure as a flexible (or semi-rigid) reinforcement. This technique can cut fabrication time and effort by eliminating the molding, curing, and adhesion process. We also reduce the fabrication hurdle by utilizing fewer materials types and less equipment, without sacrificing the variety of features.

The goal of this research is to accelerate the exploration of new soft robot applications, especially in the field of human interaction. Similar to our motivation, "Soft Robotics Toolkit" [3] is an online resource dedicated to helping soft robot researchers create and share new ideas of soft robotics technology. This toolkit which was started in 2013, has been promoting soft robots research to the children and general public. It shows how interest in soft robots are growing in recent years. Correspondingly, fast and easy prototyping techniques of soft robots are becoming essential.

Previous work in shape-changing programmable materials has proposed 4D printing [4]. 4D printing is a term when smart materials fabricated by 3D printing in a particular shape alter their given shape or properties with respect to time under the influence of some external stimuli. Recent works in soft robotics have also started utilizing 3D printing as a key technology for fabrication [5]. Although both these proposed techniques allow a convenient step to fabricate soft robots. Both of the techniques either need a high-end printer or a modified 3D printer. This need is due to materials used such as hydrogels, silicone rubbers, and shape memory polymer(SMPs) are still uncommon materials for current commercially available 3D printers. Our proposed technique, on contrary, utilized an unmodified desktop 3D printer, and common materials such as PLA and TPU. However, our technique has a shortcoming that required the assembling of PAMs into 3D printed structures.

Several works have explored the possibility of soft pneumatic actuators printed directly with an unmodified 3D printer [6], [7], [8]. These works show both the actuator's capabilities and applications in soft robots or shape-changing interfaces. However, these actuators durability and reliability are highly dependent on the 3D printer and materials used. Our prototyping technique uses pre-manufactured PMAs that can exert contraction force up to 60N under air pressure of 0.4MPa [9]. In addition, 3D printed substrate is only used for reinforcement structure, hence less material and printing time are needed.

Pneumatic artificial muscles(PAMs) such as McKibben Actuator, since patented in the 1950s have been used in many robotics applications [10]. Suzumori et al. pioneered the utilization of soft pneumatic actuators for soft robots manipulator in the 1980s [11]. In recent works, PAMs have been widely used for wearable soft robots actuator because of their lightweight and high-efficiency properties [12], [13], [14]. Although some of these previous works also utilized 3D printed reinforcement to control PAMs deformation, this paper is the first to focus on the variety of reinforcement designs and describe a novel fabrication process in detail.

While a flexible body is the main purpose of soft robots, it is also the main challenge where positioning control becomes difficult. Variable stiffness is one of the best solutions for this challenge which also exists in nature such as octopus arms and elephant trunks [15]. The most common way of variable stiffness in soft robots is the vacuum jamming technique which includes granular, layer, and fiber jamming [16], [17]. Another technique is using Low melting Point Materials (LMPMs) such as Wax and Low melting Point Alloy(LMPAs) and external stimuli such as heat and electric power [18], [19]. These stiffness control techniques are not suitable for prototyping because of the difficulty to handle different power sources for robot actuation and stiffness tuning(e.g.: compressor and vacuum pump). In this paper, we proposed a more convenient control system, where both robot actuation and variable stiffness are powered by compressed air.

Modularity on soft robots offers great advantages such as reducing the fabrication and maintenance cost, where independent modules can be easily replaced. It also offers reconfigurability, which allows soft robots to be scaled and rearranged to adapt to the environment [20]. Onal et al. proposed a modular approach to creating soft robotic systems, where the module can be arranged in series or parallel composition [21]. Other work also introduced reconfigurable soft robots, where varieties of modules are capable of different deformation (translation, bending, and twisting) [22], [23]. Similarly, this research utilizes modular structures with different kinds of features for assembling. Although the modules cannot be disassembled freely due to PAMs being threaded, both 3D printed substrate and PAMs are reusable after disassembling. Further, we propose innovative ideas to mix deformation and variable stiffness modules. We also utilize modularity to scale up robot size and actuation force.

The main goal of this research is to help soft robot researchers and enthusiasts to create prototypes fast, efficient, and inexpensive. We believe that in the current stage of soft robot development, exploring applications and interaction first will motivate the progress in core technology such as materials, actuation, sensing, and energy.

The contributions of this research are listed as follows:

1) Prototyping technique for fast and convenient soft robot fabrication using only PAMs and 3D printed reinforcement.
2) Reinforcement design for variable stiffness soft robot and the stiffness range evaluation.
3) Parallel and series arrangement of the reinforcement module, parallel application as force scaling technique, and force scaling evaluation on different module.
4) Six soft robot application examples.

II. DESIGN AND METHODS

We identify the requirements of our prototyping technique as follows:

Fast fabrication: The fabrication process of this technique must take a minimal amount of steps. And fabrication time needs to be faster than the conventional method.

Low cost and accessible: Both the equipment and materials used for fabrication must be commercially available. The minimum type of materials and equipment required, and the fabricated robot should be re-configurable and reusable for other purposes.

Simplicity: This technique needs to be intuitive, allowing the novice to understand and use the fabrication method easily. It also needs to be easy to modify and combine. Moreover, it needs to be able to scale up and scale down freely.

A. FABRICATION METHODS

To achieve a prototyping technique that meets these requirements, we design the soft robot system consisting only of 3 parts: pneumatic artificial muscles(PAMs) as actuators, 3D printed structures as reinforcement, and compressed-air controls. This section describes the fabrication process of our proposed technique and the design of both deforming and variable stiffness reinforcements.

1) 3D Printing

The key point of this technique consists in the fabrication of reinforcement structures using 3D printing. We experimented using both FDM(Fused Deposition Modeling) and SLA(Stereolithography Apparatus) 3D printers to verify this

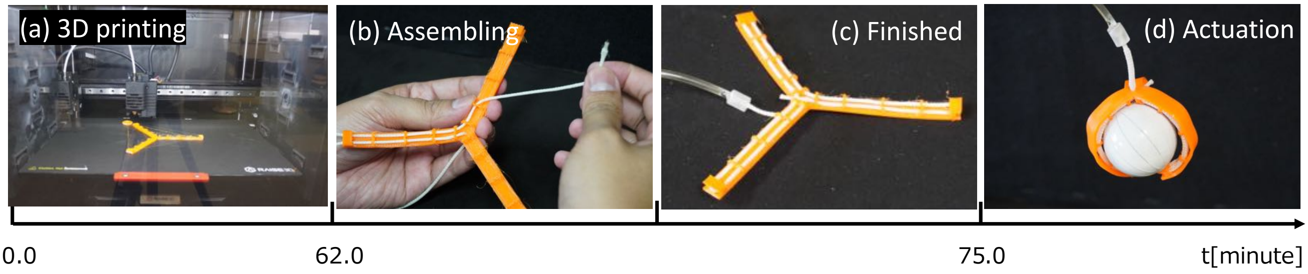

FIGURE 1. Fabrication workflow example: soft gripper.

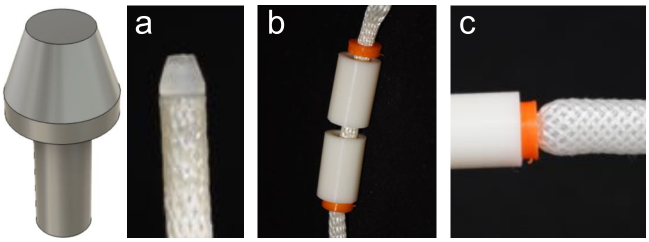

FIGURE 2. 3D printed peripherals: (a) End cap for PAMs threading. (b)(c) TPU stopper ring for reinforcements

technique's capability. Fig. 1(a) shows the Fabrication process which starts with 3D printing on FDM printer(Raised 3D). For FDM printer materials, we use PLA or ABS material for rigid reinforcement, and TPU95 (Polyflex) for flexible reinforcement. Likewise, for SLA printer(Formlab V2), we use standard resin for rigid reinforcement and FLexible 80A resin for flexible reinforcement. The 3D printer is also used to fabricate a PMAs end cap, tube connector, and stopper mechanism to keep reinforcement in place. All the 3D structures in this research are designed using commercial 3D modeling software (Fusion 360).

2) Assembling

The assembly process of our technique is similar to beads craftworks, where manual work of threading PAMs through holes on reinforcements is needed. Though this process takes time and effort, tests with several people show that most people can understand and do these procedures easily. Fig. 1(b) show the assembling process of threading PMAs. We test several PAMs end cap shapes to facilitate and reduce assembly time. And we select a cone-shaped cap with 10 mm tube inner reinforcement(See Fig. 2(a)).

To fix the end of 3D printed reinforcement to PAMS, we don't use adhesives so both 3D structure and PAMs can be collected and repurposed afterward. For this purpose, we 3D printed a flexible stopper ring with a hole size the same as the PAMs diameter. Fig. 2(b) show how we attach the stopper ring to the PAMs. This arrangement although not solidly fixing the reinforcement into PAMs. It can stop the reinforcement from moving when PAMs contract. This stopper ring can oppose the contraction force, due to the expansion of PAMs cross-section, anchoring the stopper ring in its position tightly(See Fig. 2(c)).

In this paper, we use PAMs actuator that is produced by S-muscle co. There are 3 types of size variation consisting of 1.8 mm, 3 mm, and 5 mm in outer diameter. However, to simplify the evaluation of this preliminary work, we conduct all the experiments using 5 mm PAMs. The contraction force of the 5 mm PAMs under air pressure of 0.4 MPa is approx. 60 N, and the contraction rate is approx. 25% [9]. We use 0.4 MPa as maximum pressure to prolong the PAMs usage lifetime, as the PAMs need to be reused repeatedly.

3) Pneumatic controller

In the final step of fabrication, pneumatic pressure control can be attached to the tail side of PAMs. The pressure of compressed air provided by a pump/compressor can be adjusted using an electro-pneumatic regulator with max. 1500 L/min peak flow rate capability (ITV2050-212L, SMC Corp.). Command signals to the regulator are communicated from the PC via a microcontroller and digital-analog converter(DAC, 10 bits). Fig. 1(c) shows the actuated soft gripper when applied with 0.4 MPa pressured air. In this case of small soft gripper fabrication, the total time taken to 3D print, assemble, and connect pneumatic control is 75 minutes.

B. DEFORMATION DESIGN

Deformation is achieved by altering PAMs contraction force using a variety of reinforcements. We design three types of reinforcement including bending, twisting, and contractible. Fig. 3 shows design of reinforcement for each deformation type.

1) Bending

The bending behavior is inspired by the bilayer actuation phenomenon. The basic structure of bending reinforcement is a 3D printed flexible layer with rings along the layer acting as a guide rail for PAMs actuator. The ring hole diameter is 9 mm, which is the same as PAMs maximum expansion diameter. The interval between each ring is 25mm. We design reinforcement layer thickness of approximately 3 mm to maximize the attainable bending angle.

This article has been accepted for publication in IEEE Access. This is the author's version which has not been fully edited and
content may change prior to final publication. Citation information: DOI 10.1109/ACCESS.2022.3194887

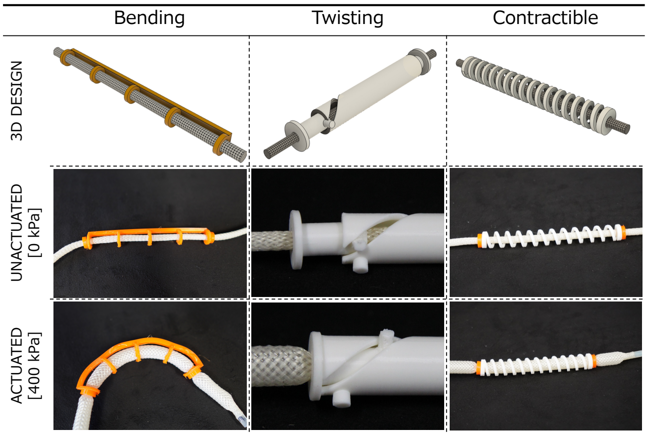

FIGURE 3. Deformation behavior related with reinforcement design

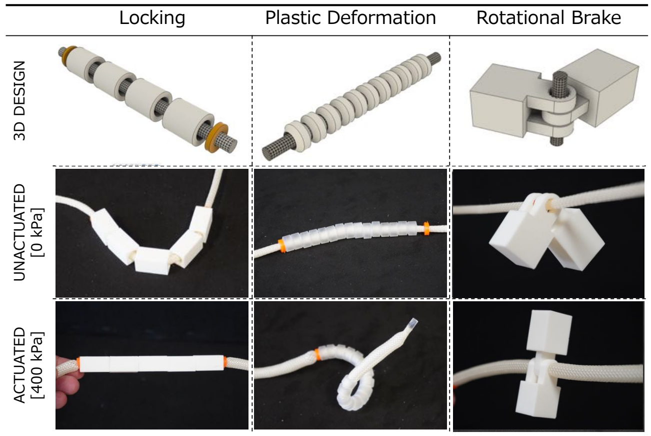

FIGURE 4. Variable stiffness behavior related with reinforcement modules

2) Twisting

The twisting behavior is inspired by the screw mechanism, converting linear motion into rotation. We design twisting reinforcement as a rigid tube, with a twisting channel on one end. The tube will rotate when another tube with protruding pin slides inside the twisting channel. Considering the contraction ratio and contraction force of our PAMs, we design the twisting channel to be 9 mm in inner diameter and 30 mm in pitch.

3) Contractible

The contractible behavior is inspired by the spring structure. Although PAMs able to contract without the spring reinforcement, the spring can store compression energy and exert opposing force. The 3D printed spring structure also adds some rigidity to PAMs soft body, while allowing flexibility in deformation. We design the spring structure to be 9 mm in inner diameter, 5 mm pitch and 2.5 mm in thickness.

C. VARIABLE STIFFNESS DESIGN

For extending interaction type and application, we design three types of variable stiffness features. Variable stiffness is achieved by altering both the contraction force and expansion force of the PAMS with 3D printed reinforcement. Fig. 4 shows 3D model of reinforcement for each variable stiffness design.

1) Locking

The locking mechanism is based on the layer jamming phenomenon. Instead of using a vacuum to change the stiffness, we use the contraction force of PAMs to compress an array of hollow reinforcement and lock it to each other[24]. The basic design of the locking module is a hollow tube with a 9 mm hole for PAMs. The modules are arranged in series, threaded with PAMs, and attached with stoppers at both ends. The locking module can be 3D printed in any form, and the module segment can be printed at an angle to allow deformation such as shearing(see Fig. 5(a)).

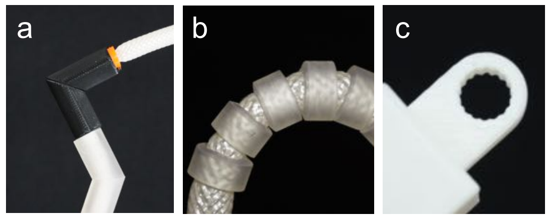

FIGURE 5. (a) 90°shear deformation as result of angled segment. (b) Bulge between plastic deformation modules. (c) Gear tooth to increase brake torque

2) Plastic deformation

Plastic deformation behavior allows the structure retains its shape after being bent by an external force. Similar to locking, plastic deformation structure also comprises hollow reinforcement arranged in series. The key difference between plastic deformation and locking module is the 7 mm hole size, which is smaller than the PAMs diameter when expanded. Due to this, the module will stick to PAMs when PAMS is actuated. And when the structure is bent, PAMs will bulge out on a small gap between modules(see Fig. 5(b)). This bulge allows the structure retains its shape and becomes deformable. To increase the range of bending angle, We also add a 45°chamfering edge into the plastic modules.

3) Rotational brake

The rotational brake mechanism is based on a hinge structure with PAMs as its shaft. When PAMs is unactuated, the hinge can rotate freely. However, when PAMs are expanded inside the hinge, they will rub together and resist rotation. We design the hinge hole to be 7 mm in size, and add a gear tooth into the hole to increase the brake torque(see Fig. 5(c))

D. CORRELATION BETWEEN LOCKING AND PLASTIC DEFORMATION

Both locking and plastic deformation consist of a hollow module array, however with different hole diameters. In this experiment, we investigate the relationship between hole diameter and deformation behavior. We measure the three-

This article has been accepted for publication in IEEE Access. This is the author's version which has not been fully edited and
content may change prior to final publication. Citation information: DOI 10.1109/ACCESS.2022.3194887

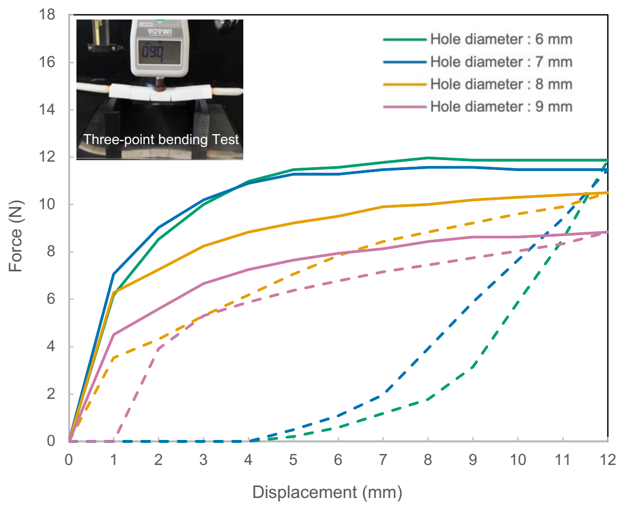

FIGURE 6. Stress-strain graph by three-point bending test. The coloured lines represent loading phase on different hole diameter. Dashed line represent hysteresis loop on unloading phase

point bending of hollow modules with variation in hole diameter. The pressure is set at 0.4 MPa and we measure load for every 1 mm displacement. Fig. 6 shows the forces reduce as the hole diameter increases. However, unloading phase hysteresis (dashed lines) shows each hole diameter exhibits different behavior. The 9 mm and 8 mm holes both exhibit elastic behavior, and the 6 mm and 7 mm holes exhibit plastic behavior. Based on these results, we select the 9 mm hole for locking modules to maximize the elasticity when applied with a load. For plastic deformation modules, we select the 7 mm hole because the properties are similar to the 6 mm hole, while the assembly is easier for threading the PAMs.

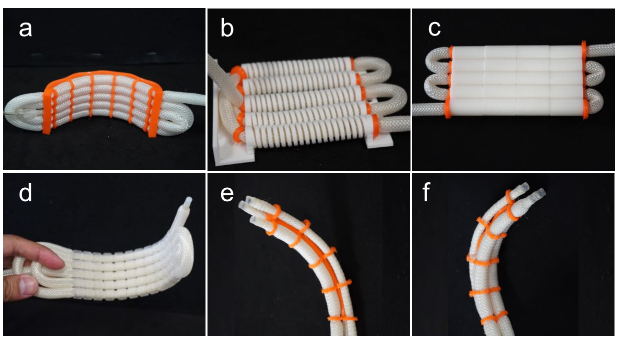

FIGURE 7. Parallel arrangement: (a) Bending, (b) Contractible, (c) Locking, (d) Plastic deformation, (e)(f) Three chambered actuator on different actuation phase.

III. RESULTS

A. COMBINATION OF REINFORCEMENTS

Our prototyping technique provides a total of six reinforcement features with elongated shapes along the PAMs. Because of this simple one-dimensional shape, each feature is compatible to be arranged both in series and parallel.

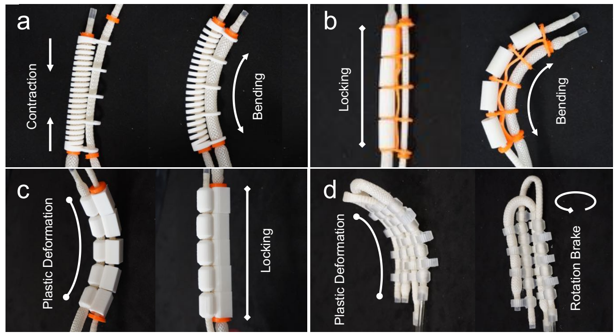

FIGURE 8. Parallel mixing example: (a) contraction-bending, (b) locking-bending , (c) plastic-locking , (d) plastic deformation-rotational brake.

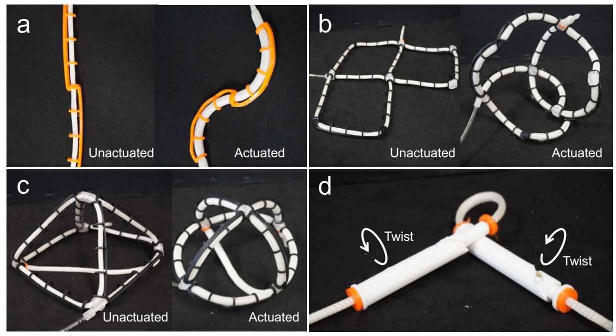

FIGURE 9. Series arrangement: (a) S-shaped Bending, (b) 2D structure, (c) 3D structure, (d) Twisting module bonded on moving part of another twisting.

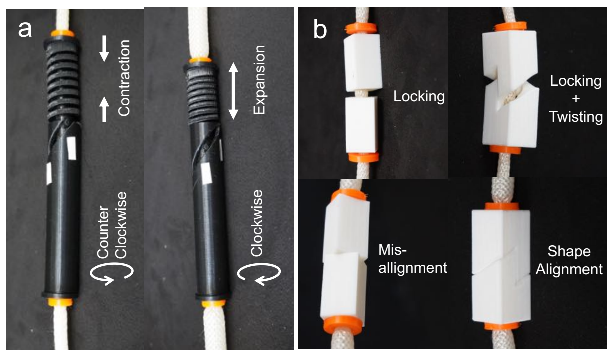

FIGURE 10. Series mixing example: (a) contractible-twisting, (b) locking-twisting.

Moreover, the modularity of the structure grants flexibility for mixing arrangements between the features.

1) Parallel arrangement

A parallel arrangement of same the features allows scalability of PAMs contraction force. This arrangement can create a stronger bending force, a stronger contractible spring, a stiffer locking, and stiffer plastic deformation (Fig. 7(a)(b)(c)(d)). This parallel arrangement can also be utilized to navigate the bending direction by arranging the bending module in a three-chambered structure(see Fig. 7(e)).

Mixing between features in a parallel arrangement allows for multiple behaviors in one structure. For example, mixing between contractible and bending allows deformation that mimics earthworm crawling gait (Fig. 8(a)). Mixing between bending and locking allows stiffening of the flexible bending reinforcement, similar to octopus tentacle or elephant trunk ability(Fig. 8(b)). Another example such as locking-plastic deformation mixing, and plastic deformation-rotational brake mixing allows deformability of structure shapes (Fig. 8(c)(d)).

2) Series arrangement

Series arrangement of the same features allows scalability of the structure dimensions. It scales the structural length of the basic module. However, when configured in a two-dimensional or three-dimensional arrangement, It scales the area and volume of the structures(Fig. 9(b)(c)). Other utilization are including alternate bending directions and a complex twisting movement where a twist module is attached to a moving part of another twisting module (see Fig. 9(a)(d)).

Mixing between features in a series arrangement can create a new and unique trait with practical utilization. For example, mixing between contractible and twisting allows a reversible twisting motion, where it rotates when PAMs are actuated and reverses the rotation when the spring is extended (Fig. 10(a)). Another example is mixing between twisting and locking which allows shape-memory properties of the module alignment(see Fig. 10(b)). Hence, the locking position does not need to be realigned every time the PAMs are actuated.

B. VARIABLE STIFFNESS VERIFICATION

Stiffness variation in locking, plastic deformation, and rotational brake modules is determined by contraction and radial expansion of PAMs. Since both contraction ratio and expansion ratio are influenced by air pressure. Thus, we can control the stiffness of each module by adjusting the air pressure. In this section, we verify the relationship between

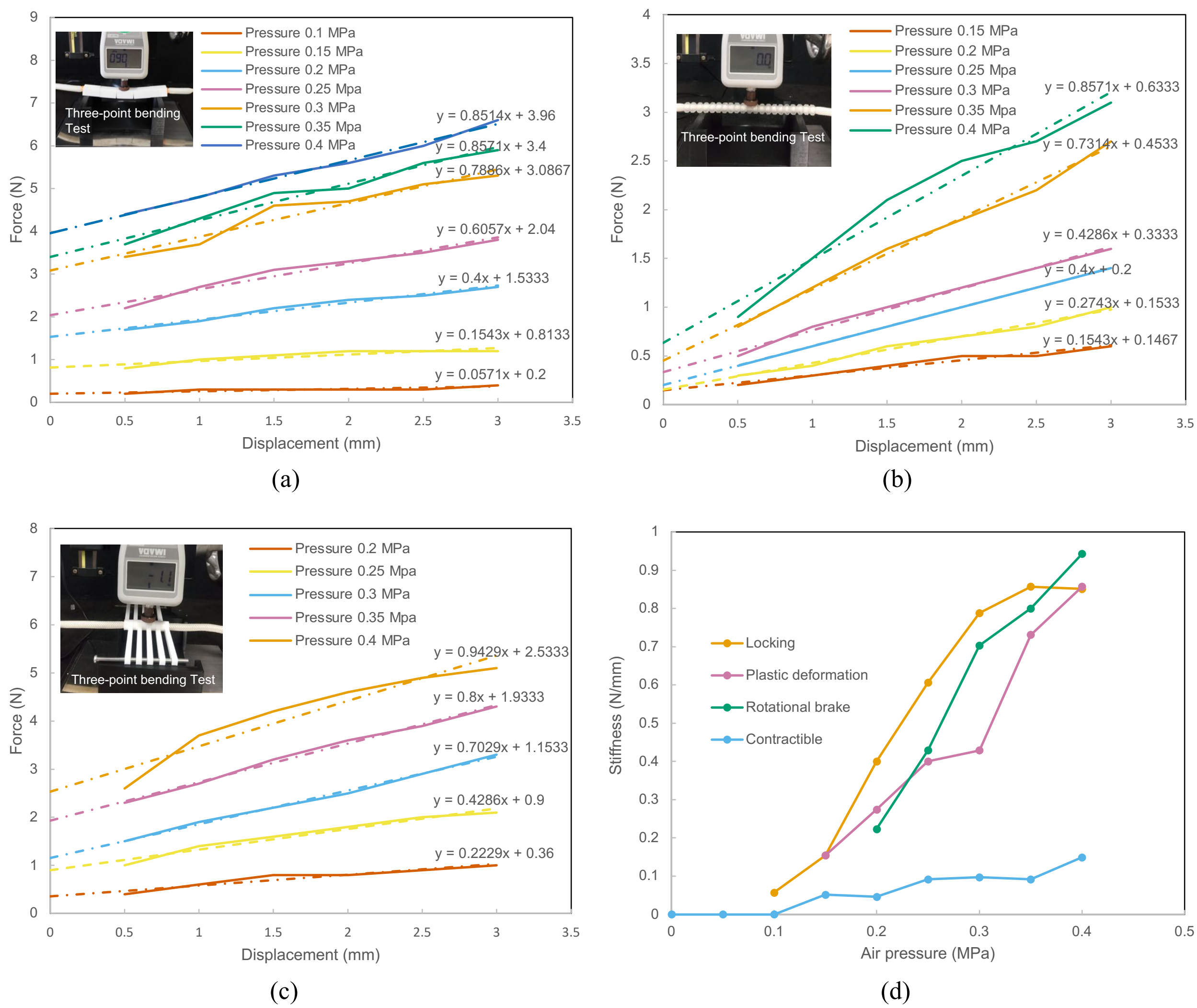

FIGURE 11. Stress-strain graph : (a) Locking, (b) Plastic deformation, (c) Rotational brake. (d) Relationship between air pressure and module stiffness

This article has been accepted for publication in IEEE Access. This is the author's version which has not been fully edited and
content may change prior to final publication. Citation information: DOI 10.1109/ACCESS.2022.3194887

the stiffness of the modules and the air pressures.

Fig. 11(a)(b)(c) shows stress-strain curves in a three-point bending flexural test, on locking, plastic deformation, and rotational brake reinforcements. The applied pressure was varied in 0.05MPa steps from 0 MPa to 0.4 MPa, and we found that the locking mechanism shows a stiffness change from 0.1 MPa, while plastic deformation and rotational brake showed stiffness change from 0.15 MPa and 0.2 MPa respectively. The dash-dotted line shows the line fitting with the approximation formula. All the modules show increases in force as the air pressure increases, with the locking module showing the highest force.

Fig. 11 (d) shows the stiffness change according to the air pressure variation on each reinforcement module. It shows non-linear increases in stiffness as the air pressure increases. Each module has a different range of stiffness variation, with the rotational brake module having the highest stiffness of 0.94 N/mm. And locking modules show the widest stiffness range from 0.06 N/mm up to 0.86 N/mm. We also added stiffness measurement of contractible modules as a comparison, which shows the stiffness change on the PAMs itself.

C. FORCE SCALING VERIFICATION

The conventional way of increasing PAMs contraction force is by using bigger PAMs with a larger cross-sectional area. Previous work has proven that multifilament PAMs structure is also an effective way to scale contraction force[25]. We introduce a similar scaling technique, however using only one long PAMs filament arranged in a zigzag loop(see Fig. 7). This technique allows convenient scaling implementation, with less effort in creating multiple air-supply connections. In this section, we verify the effectiveness of our force scaling technique and its compatibility with four types of reinforcement design.

1) Spring contractible scaling

Fig. 12(a) shows relationship between applied air-pressure and contraction force on contractible structure. The Contraction force increase along with applied pressure. The contraction force also increases proportionally with the number of parallel PAMs filaments. The maximum contraction force of 5 filaments is 111 N when the applied pressure is 0.4 MPa.

Fig. 12(b) shows the measurement of contraction force and the amount of contraction, where the applied air pressure is 0.4 MPa. This figure shows proportional scaling in contraction force, however a different trends in contraction ratio. It also achieves the maximum contraction ratio of only 14% while the PAMs specification is 25%. Both are due to the spring stiffness that resists the PAMs contraction force and the parallel arrangement that is not symmetrical.

2) Bending force scaling

Fig. 13(a) shows the relationship between applied air pressure and bending force on a parallel bending arrangement. The contraction force increase as the number of PAMs filament increases, however not proportionally. The maximum

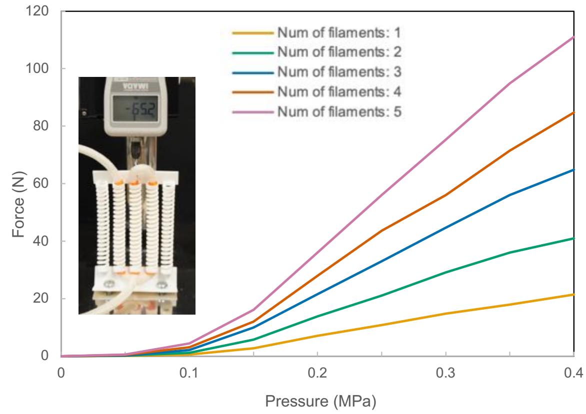

(a)

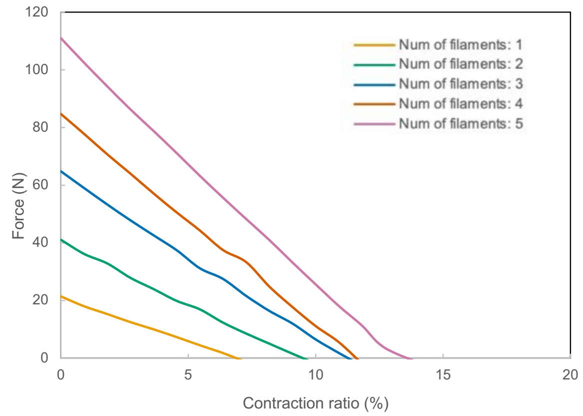

(b)

FIGURE 12. Contractible scalability: (a) Relationship between applied pressure and contraction force. (b) Relationship between contraction ratio and contraction force. The applied pressure is 0.4 MPa

bending force of 5 filaments is 10.9 N when the applied pressure is 0.4 MPa.

Fig. 13(b) shows the three-point bending test on bending structure in an arched state. It shows a trend of increase in bending force similar to the Fig. 13(a). The hysteresis loop in the dotted line shows reduces in elastic behavior as the number of filaments increases.

3) Locking stiffness scaling

A stiffer locking mechanism is advantageous to increase structural strength when withstanding heavy load. Fig. 14 shows a three-point bending test of locking structure with variation in the number of PAMs filament. This figure shows that the strength of the locking structure is nearly proportional to the number of PAMs filaments. The hysteresis loop also shows that the structure always exhibits elastic behavior even when scaled up to 5 filaments.

4) Plastic malleability scaling

Fig. 15 shows three-point bending test on plastic deformation structure. Although not proportional, it shows a stiffness increase along with an increase in the number of PAMs

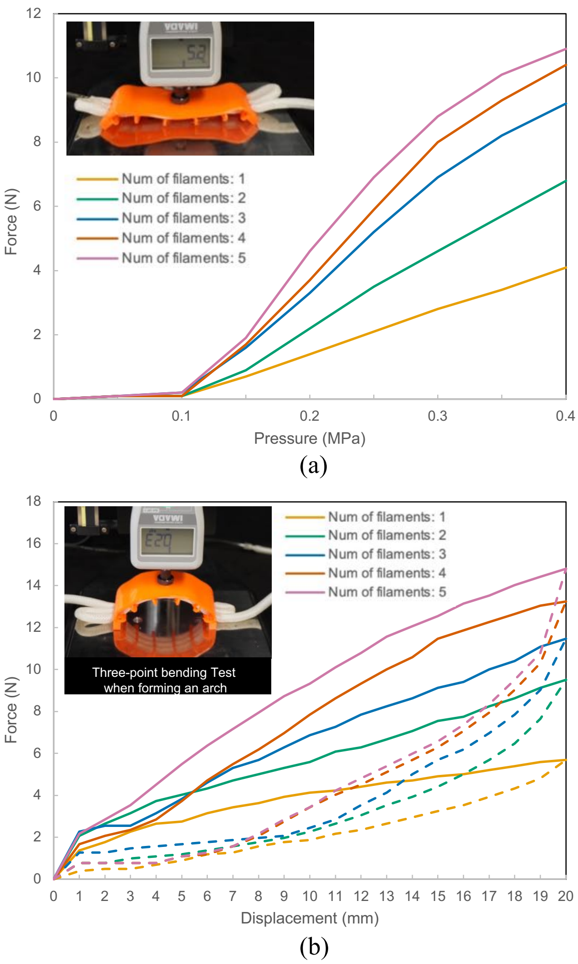

FIGURE 13. Bending scalabillity: (a) Relationship between applied pressure and bending force, (b) Three-point bending test on arched state, with 0.4 MPA applied pressure.

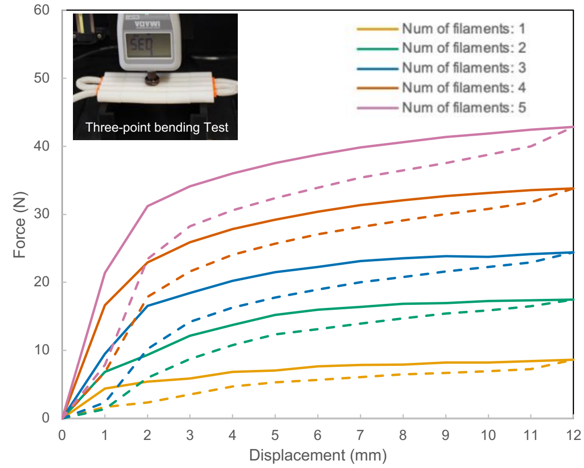

FIGURE 14. Locking scalabillity: Three-point bending test, with 0.4 MPA applied pressure.

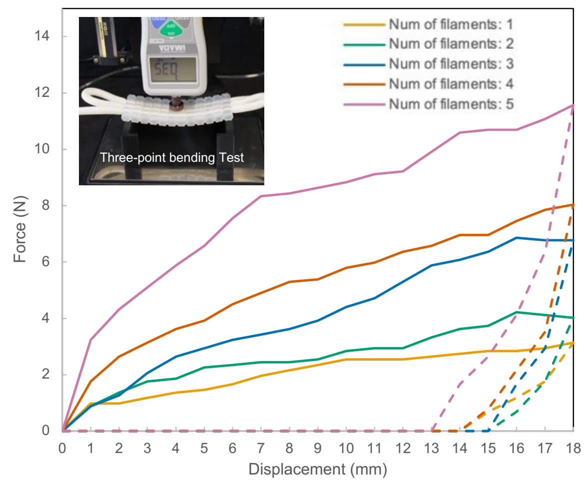

FIGURE 15. Plastic deformation scalabillity: Three-point bending test, with 0.4 MPA applied pressure.

filament. It also shows plastic behavior even when scaled up to 5 filaments. However, when scaled up, due to the increase in surface area, the structure is no longer bendable on more than one axis.

D. APPLICATION

Here, we demonstrate the application achieved through our prototyping technique. Fig. 16(a) shows a soft gripper consisting of two fingers of bending reinforcement and additional locking features on the fingertip and base. This locking feature adds controllable stiffness to the fingertip, allowing increases in positioning accuracy when picking a small object (15 mm diameter). Although it has a drawback which reduces a degree of flexibility, it is still able to grasp large objects up to 120 mm in diameter. Fig. 16(b) shows another sample of a gripper that has locking feature along the finger. When actuated, the locking mechanism allows the gripper to hold three times heavier objects compared with only the bending actuation.

Fig. 16(c) shows an example implementation of snake-like robot with variable stiffness properties. For joint between segments in the snake body, we use rotation brake features so it can retain the last posture applied. To allow both yaw and pitch rotation, we implement a hinge structure at a 90-degree angle on both sides of a module. The combined 15 modules can achieve a redundant body posture.

The third application shown in Fig. 16(d) is a crawling robot with four legs, inspired by works by Tang et al. [26]. We implement a parallel arrangement of bending reinforcement for spine structure, capable of flexion and extension motion. We use two different phases to control the spine movement, thus allowing forward locomotion.

As a wearable device example, Fig. 16(e) shows a sunglasses application. It can automatically adjust the temple length using contractible reinforcement. It is also capable of flipping up the lenses using twisting reinforcement.

Fig. 16(f) shows an example implementation of structured fabric with variable stiffness. The fabric is soft and flexible

This article has been accepted for publication in IEEE Access. This is the author's version which has not been fully edited and content may change prior to final publication. Citation information: DOI 10.1109/ACCESS.2022.3194887

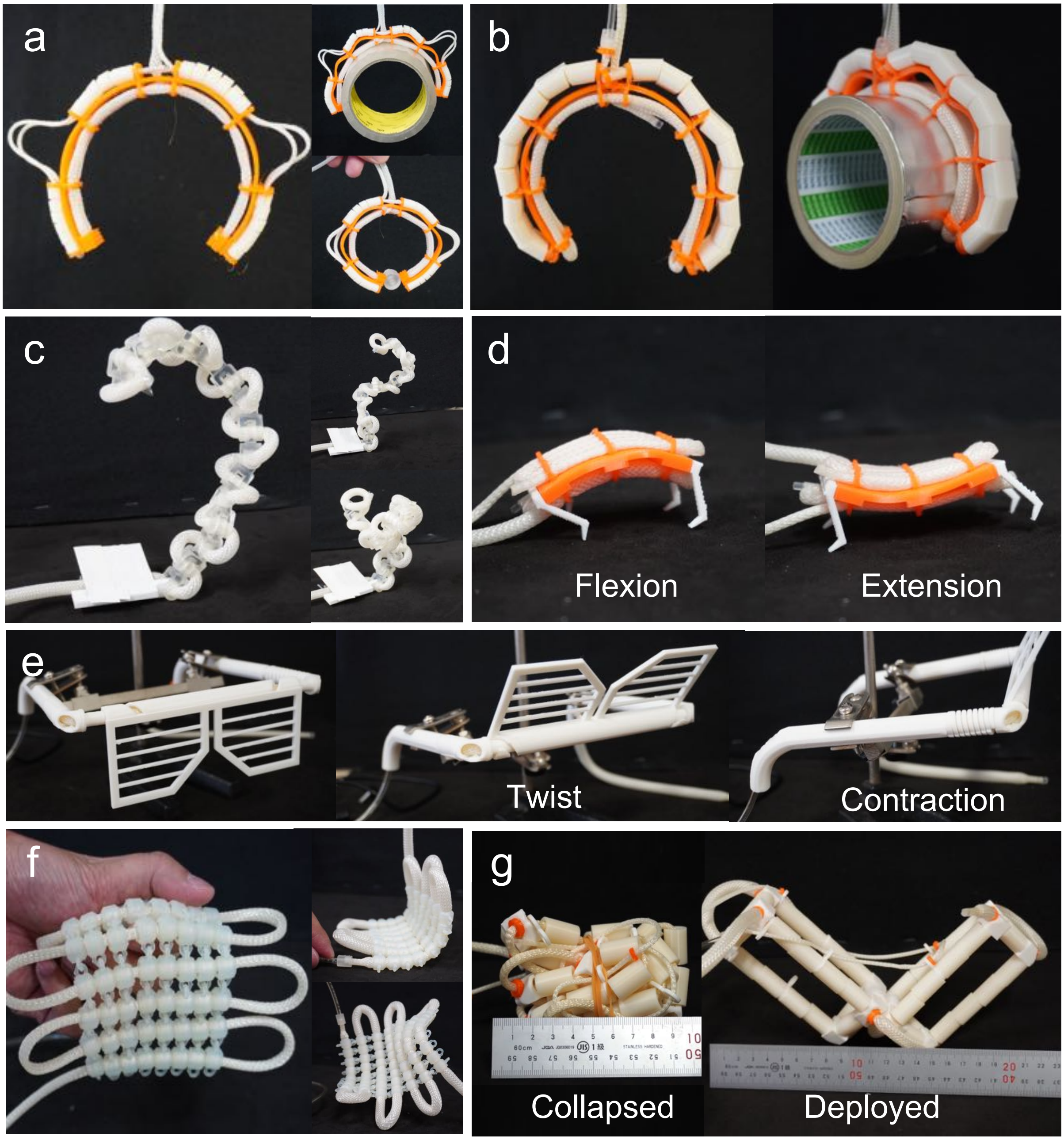

FIGURE 16. Application example: (a)(b) Soft gripper with variable stiffness. (c) Snake-shaped malleable robot. (d) Spine actuation for four-legs locomotion. (e) Wearable sunglasses, (f) Variable stiffness fabric, (g) Deployable robot

in the normal state, and malleable when actuated. Inspired by Wang et al., It consists of a plastic deformation module that is linked with chain structure in parallel arrangement [27]. It can be bent both head-on and sideway, it also can be twisted and will retain the shapes when actuated.

Fig. 16(g) shows an implementation of a deployable robot arm. Inspired by FlexTruss [28], we create two truss structures for the robot arm using the locking modules. We then joint the two arms using a hinge and add bending features into the hinge to allow manipulation. In an unactuated state, the robot arm can be collapsed into a 100 x 50 x 50 mm size.

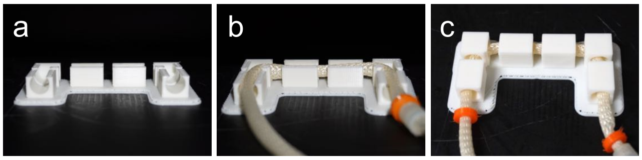

FIGURE 17. Manufacturing Solution to prevent human error and reduce assembly time

When deployed the robot will double its size, approx. 200 x 100 x 100 mm.

IV. DISCUSSION

We present a prototyping technique to decrease the time, expense, and difficulty of soft robot fabrication. We describe six designs of 3D printed reinforcements for PAMs actuated soft robots. As a preliminary report, this paper includes only basic design and combination ideas of the reinforcement. However, to facilitate more complex manipulation and larger structures, computer-aided design tools will be essential in the future. Recent work by Maloisel et al. shows a computational approach for routing PAMs through soft robots[29]. Similar to this work, computational simulation can be utilized to design reinforcement thickness to achieve desired bending deformation.

This research prototyping technique is not suited for manufacturing because manual assembling works of threading PAMs brings a lot of shortcomings. Number one is human error which often occurred when the structures become more complex. Another weakness is tedious and time-consuming PAMs threading work. One of the solutions is to create software that guides the assembling process step by step. Another approach is to stop the 3D printing process before the PAMs threading hole is closed up(Fig. 17(a)). Then PAMs can be laid in place easily along with the pre-arranged modules(Fig. 17(b)). Finally, the hole can be closed by continuing the printing process (Fig. 17(c)). In the future, this procedure can be automated by a robotic arm and conveyor belt on a 3D printer.

In this paper, we verify both the variable stiffness and force scaling capabilities through experiments. However other quantitative experiments such as bending angle, shearing angle, twisting angle, and shape deformability are yet to be explored. In this paper, we also only study the relation of stiffness change with air pressure. However, other parameters that also influence the stiffness such as hole diameter, hole texture, and surface area are yet to be explored. This property can be used to varying the stiffness of different robot parts, even when the same pressure is applied.

We emphasize the advantage of using only one filament for easier assembling and control simplicity. However, it also has drawbacks such as a long actuation time due to a non-parallel tube connection. It is also difficult to disassemble and reconfigure due to no joint that can be detached. As a solution, we plan to implement a small connector (smaller than the PAMs diameter) that can be threaded along with the PAMs. Similar to the approach by Kwok et al. [30], a ring-shaped magnet can be utilized as a connector.

We envision our prototyping technique can be useful in soft robot exploration. Researchers and enthusiasts can create working prototypes easily, rapidly, and at a low cost. Along with discoveries of soft robot application and utilization, we believe this research can be developed further to be soft robot manufacturing technology.

REFERENCES

[1] G. M. Whitesides, “Soft-robotik,” *Angewandte Chemie*, vol. 130, pp. 4336–4353, 4 2018.

[2] F. Schmitt, O. Piccin, L. Barbé, and B. Bayle, “Soft robots manufacturing: A review,” *Frontiers Robotics AI*, vol. 5, 2018.

[3] D. P. Holland, E. J. Park, P. Polygerinos, G. J. Bennett, and C. J. Walsh, “The soft robotics toolkit: Shared resources for research and design,” *Soft Robotics*, vol. 1, pp. 224–230, 9 2014.

[4] S. Tibbits, “4d printing: Multi-material shape change,” *Architectural Design*, vol. 84, pp. 116–121, 1 2014.

[5] J. Z. Gul, M. Sajid, M. M. Rehman, G. U. Siddiqui, I. Shah, K. H. Kim, J. W. Lee, and K. H. Choi, “3d printing for soft robotics–a review,” *Science and Technology of Advanced Materials*, vol. 19, pp. 243–262, 12 2018.

[6] J. Morrow, S. Hemleben, and Y. Menguc, “Directly fabricating soft robotic actuators with an open-source 3-d printer,” *IEEE Robotics and Automation Letters*, vol. 2, pp. 277–281, 1 2017.

[7] H. Kim, A. Everitt, C. Tejada, M. Zhong, and D. Ashbrook, “Morpheesplug: A toolkit for prototyping shape-changing interfaces,” *Proceedings of the 2021 CHI Conference on Human Factors in Computing Systems*, pp. 1–13, 5 2021.

[8] B. N. Peele, T. J. Wallin, H. Zhao, and R. F. Shepherd, “3d printing antagonistic systems of artificial muscle using projection stereolithography,” *Bioinspiration and Biomimetics*, vol. 10, 9 2015.

[9] S. Kurumaya, H. Nabae, G. Endo, and K. Suzumori, “Design of thin mckibben muscle and multifilament structure,” *Sensors and Actuators, A: Physical*, vol. 261, pp. 66–74, 7 2017.

[10] D. Trivedi, C. D. Rahn, W. M. Kier, and I. D. Walker, “Soft robotics: Biological inspiration, state of the art, and future research,” *Applied Bionics and Biomechanics*, vol. 5, pp. 99–117, 2008.

[11] K. Suzumori, S. Iikura, and H. Tanaka, “Flexible microactuator for miniature robots,” *[1991] Proceedings. IEEE Micro Electro Mechanical Systems*, pp. 204–209, 1991.

[12] N. Takahashi, S. Furuya, and H. Koike, “Soft exoskeleton glove with human anatomical architecture: Production of dexterous finger movements and skillful piano performance,” *IEEE Transactions on Haptics*, vol. 13, pp. 679–690, 10 2020.

[13] Y. Funabora, “Prototype of a fabric actuator with multiple thin artificial muscles for wearable assistive devices,” *SII 2017 - 2017 IEEE/SICE International Symposium on System Integration*, vol. 2018-January, pp. 356–361, 2 2018.

[14] M. Tschiersky, E. E. Hekman, D. M. Brouwer, J. L. Herder, and K. Suzumori, “A compact mckibben muscle based bending actuator for close-to-body application in assistive wearable robots,” *IEEE Robotics and Automation Letters*, vol. 5, pp. 3042–3049, 4 2020.

[15] M. Manti, V. Cacucciolo, and M. Cianchetti, “Stiffening in soft robotics: A review of the state of the art,” *IEEE*

This article has been accepted for publication in IEEE Access. This is the author's version which has not been fully edited and content may change prior to final publication. Citation information: DOI 10.1109/ACCESS.2022.3194887

Robotics and Automation Magazine, vol. 23, pp. 93–106, 9 2016.

[16] J. R. Amend, E. Brown, N. Rodenberg, H. M. Jaeger, and H. Lipson, "A positive pressure universal gripper based on the jamming of granular material," *IEEE Transactions on Robotics*, vol. 28, pp. 341–350, 4 2012.

[17] Y.-J. Kim, S. Cheng, S. Kim, and K. Iagnemma, "Design of a tubular snake-like manipulator with stiffening capability by layer jamming," *2012 IEEE/RSJ International Conference on Intelligent Robots and Systems*, pp. 4251–4256, 10 2012.

[18] J. Shintake, B. Schubert, S. Rosset, H. Shea, and D. Floreano, "Variable stiffness actuator for soft robotics using dielectric elastomer and low-melting-point alloy," *2015 IEEE/RSJ International Conference on Intelligent Robots and Systems (IROS)*, vol. 2015-December, pp. 1097–1102, 9 2015.

[19] N. G. Cheng, A. Gopinath, L. Wang, K. Iagnemma, and A. E. Hosoi, "Thermally tunable, self-healing composites for soft robotic applications," *Macromolecular Materials and Engineering*, vol. 299, pp. 1279–1284, 11 2014.

[20] C. Zhang, P. Zhu, Y. Lin, Z. Jiao, and J. Zou, "Modular soft robotics: Modular units, connection mechanisms, and applications," *Advanced Intelligent Systems*, vol. 2, p. 1900166, 6 2020.

[21] C. D. Onal and D. Rus, "A modular approach to soft robots," in *2012 4th IEEE RAS EMBS International Conference on Biomedical Robotics and Biomechatronics (BioRob)*, 2012, pp. 1038–1045.

[22] J. Y. Lee, W. B. Kim, W. Y. Choi, and K. J. Cho, "Soft robotic blocks: Introducing sobl, a fast-build modularized design block," *IEEE Robotics and Automation Magazine*, vol. 23, pp. 30–41, 9 2016.

[23] J. Ogawa, T. Mori, Y. Watanabe, M. Kawakami, M. N. I. Shiblee, and H. Furukawa, "Mori-a: Soft vacuum-actuated module with 3d-printable deformation structure," *IEEE Robotics and Automation Letters*, vol. 7, pp. 2495–2502, 4 2022.

[24] A. Degani, H. Choset, A. Wolf, and M. Zenati, "Highly articulated robotic probe for minimally invasive surgery," in *Proceedings IEEE International Conference on Robotics and Automation. ICRA 2006.*, 2006, pp. 4167–4172.

[25] S. Kurumaya, K. Suzumori, H. Nabae, and S. Wakimoto, "Musculoskeletal lower-limb robot driven by multifilament muscles," *ROBOMECH Journal*, vol. 3, 12 2016.

[26] Y. Tang, Y. Chi, J. Sun, T.-H. Huang, O. H. Maghsoudi, A. Spence, J. Zhao, H. Su, and J. Yin, "Leveraging elastic instabilities for amplified performance: Spine-inspired high-speed and high-force soft robots," *Science Advances*, vol. 6, no. 19, 2020.

[27] Y. Wang, L. Li, D. Hofmann, J. E. Andrade, and C. Daraio, "Structured fabrics with tunable mechanical properties," *Nature*, vol. 596, pp. 238–243, 8 2021.

[28] L. Sun, J. Li, Y. Chen, Y. Yang, Z. Yu, D. Luo, J. Gu, L. Yao, Y. Tao, and G. Wang, "Flextruss: A computational threading method for multi-material, multi-form and multi-use prototyping," in *Proceedings of the 2021 CHI Conference on Human Factors in Computing Systems*, ser. CHI '21. New York, NY, USA: Association for Computing Machinery, 2021.

[29] G. Maloisel, E. Knoop, C. Schumacher, and M. Bacher, "Automated routing of muscle fibers for soft robots," *IEEE Transactions on Robotics*, vol. 37, pp. 996–1008, 6 2021.

[30] S. W. Kwok, S. A. Morin, B. Mosadegh, J. H. So, R. F. Shepherd, R. V. Martinez, B. Smith, F. C. Simeone, A. A. Stokes, and G. M. Whitesides, "Magnetic assembly of soft robots with hard components," *Advanced Functional Materials*, vol. 24, pp. 2180–2187, 4 2014.

JEFFERSON PARDOMUAN received the M.E. degree from University of Electro-Communications, Tokyo. He is currently pursuing the Ph.D. degree in computer science at Tokyo Institute of Technology. His research interests include shape-changing interfaces, soft robotics, and human augmentation.

NOBUHIRO TAKAHASHI is currently a Researcher with the Tokyo Institute of Technology, Tokyo, Japan. His research interests include tactile/haptic interfaces, humanoid robots, and soft robotics.

HIDEKI KOIKE received the B.E., M.E., and Dr. Eng. from the University of Tokyo, in 1986, 1988, and 1991, respectively. After working with the University of Electro-Communications, Tokyo, he joined Tokyo Institute of Technology, in 2014, where he is currently a Professor in the School of Computing. His research interests include vision-based HCI, human augmentation, information visualization, and usable security.

• • •